Если возмущающие моменты $M_x(u_x, u_z, n)$ и $M_{y_1}(u_{y_1}, u_{y_1}, n)$ определены, то реакция отдельных каналов гиростабилизатора определяется так же, как в случае одноосного гиростабилизатора.

Составляющие собственной скорости прецессии ω_0, ω_1, ω_2, вызванные действием вредных моментов вокруг осей прецессии, определяются для каждого канала стабилизации раздельно таким же образом, как и в случае одноосного стабилизатора. Для их уменьшения применяются различные конструктивные меры (гидростатическая разгрузка опор, применение трехколечных шарикоподшипников, создание равножестких гиромоторов со стабильным положением центра тяжести и т. д.).

Динамическую составляющую собственной скорости прецессии для каждого канала можно определить с помощью кинематической теоремы, зная абсолютный угол прецессии и угловую скорость поворота вокруг оси ротора. Для рассматриваемой схемы двухосного стабилизатора при малых μ_0 и ε_0 значение абсолютного угла прецессии определяется возмущающими моментами относительно оси стабилизации и структурой контура разгрузки, а скорость поворота вдоль оси ротора равна переносной угловой скорости вдоль оси z платформы. Наличие значительной переносной угловой скорости вокруг осей роторов вызывает большие динамические погрешности. В каждом канале их величину определяют по формулам (VIII.45), (VIII.46).

Для уменьшения динамической составляющей собственной скорости прецессии следует уменьшить переносную угловую скорость вдоль осей роторов гиромоторов. С этой целью можно использовать схему двухосного гиростабилизатора, в которой векторы кинетических моментов гироскопов лежат в стабилизированной плоскости платформы. В этом случае оси прецессии гироскопов параллельны стабилизированной оси z платформы.

Недостатком такой схемы является наличие возмущений в контуре разгрузки при переносном движении вокруг оси z платформы.

Снижение погрешностей гиростабилизатора, представленного на рис. VIII.11, может быть получено в случае применения четырехгироскопного гиростабилизатора.

Рабочий угол α_0 наружной оси кардана двухосного гиростабилизатора принципиально не ограничен. Угол поворота по внутренней оси кардана β_0 обычно не превышает 45°—60°, так как с увеличением угла β_0 снижается нутационная частота и возрастает пропорционально $\operatorname{tg}\beta_0$ инерционный момент от платформы и рамы кардана, возникающий при угловых ускорениях вокруг оси, перпендикулярной плоскости наружной рамы [8].

5. ТРЕХОСНЫЕ, ИЛИ ПРОСТРАНСТВЕННЫЕ, ГИРОСКОПИЧЕСКИЕ СТАБИЛИЗАТОРЫ

Трехосные гиростабилизаторы служат для угловой стабилизации различных устройств в пространстве. Трехосные гиростабилизаторы строятся с использованием принципа силовой гироскопи-

<< Previous paragraph Next paragraph >>

253 254 255 256 257 258 259 260 261 262 263 264 265 266 267 268 269

Page layouts

5. THREE-AXIAL OR SPATIAL GYROSCOPIC STABILIZERS

Triaxial gyro stabilizers are used for angular stabilization of various devices in space. Triaxial gyrostabilizers are built using the principle of force gyroscopic

stabilization and indicator-power (indicator) stabilization.

Three-axis gyrostabilizers are used as central sensing devices for autopilots for heading, roll and pitch of an aircraft, in inertial navigation systems and for stabilizing homing antennas.

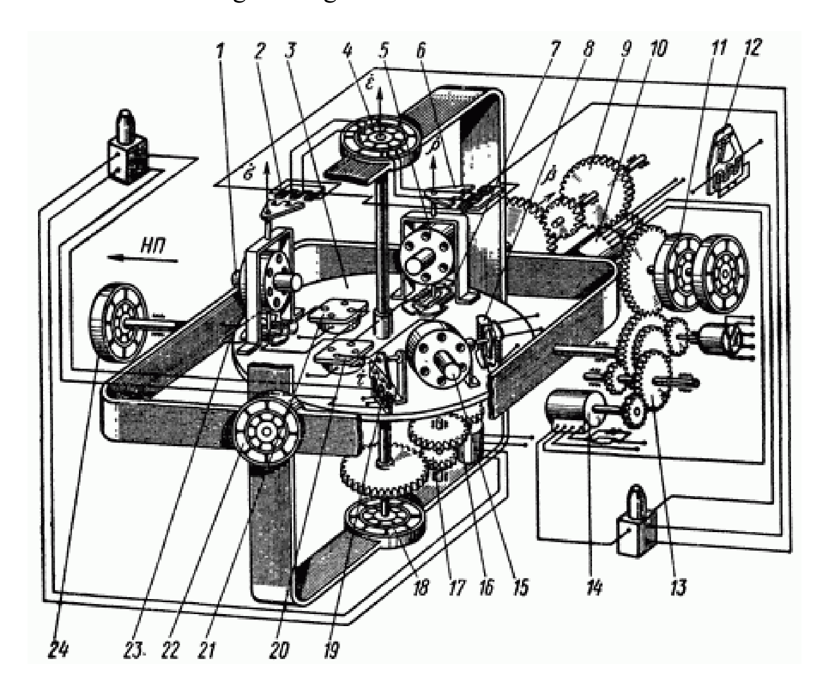


Fig. VIII. 12. Kinematic diagram of the sensor of the heading, roll and pitch angles of the autopilot: 1 - gyroscope ; 2 - inductive sensor; 3 - platform; 4 - coordinate converter; 5 - gyroscope; 6 - inductive sensor; 7.8 - correcting torque sensors; 9 - reducer; 10 - unloading motor; II - bend mechanism; 12 - bendable pendulum; 13 - reducer; 14 - unloading motor; 15 - gyroscope; 16 - unloading motor; 17 - reducer; 18 - selsyn-sensor; 19 - inductive sensor; 20, 21 - liquid switches; 22 - selsyn-sensor; 23 - correcting torque sensor; 24 - selsyn-sensor

Compared to a biaxial gyro stabilizer, a spatial gyro stabilizer differs in that its platform has complete freedom of rotation (three degrees of freedom) relative to the device body. The angles of rotation of the platform around the axes of the inner and outer frames of the gimbal suspension are not limited, while the angle of rotation of the platform around the middle axis, due to the same factors that take place in a biaxial gyro stabilizer, usually does not exceed 45 ° -60 °.

Power gyro stabilizer. The scheme of the power spatial gyroscopic stabilizer, which is the central

the heading and elevation sensor of the autopilot, shown in Fig. VIII.12. The main part of the device is platform 3, mounted in a gimbal, with gyroscopes, correction devices and angle sensors. Platform 3 serves as a base for three gyroscopes 1, 5, 15, having two degrees of freedom relative to the platform. Corrective torque sensors 7, 8, 23 and inductive sensors 2,6 and 19 of the gyroscopes rotation angles relative to the platform are installed on the precession axes of each of the gyroscopes. Liquid pendulum switches 20 and 21 are also installed on the platform, correcting the position of the platform in relation to the plane of the horizon.

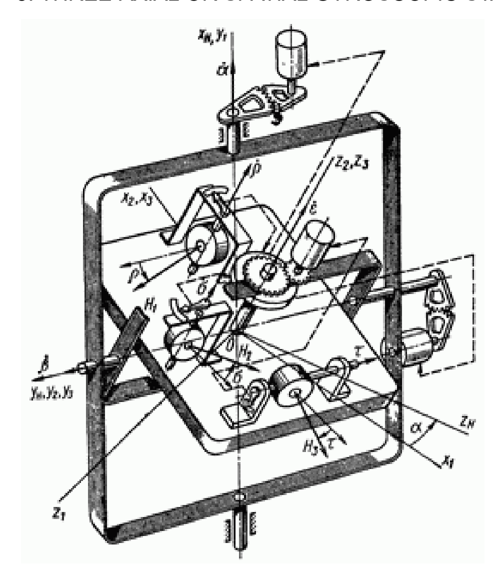


Fig. VIII. 13. Schematic diagram of a triaxial gyro stabilizer

The gyroscopic stabilizer shown in Fig. VIII. 12 allows using sensors 18, 22 and 24 to determine the angles of the course, roll and pitch of the aircraft without cardan error.

To compose the equations of motion of the gyrostabilizer (uncorrected by the corrector pendulum), we will use Fig. VIII. 13, which shows the corresponding coordinate axes defining the position of the gyro-stabilizer platform and the aircraft in space. We place the origin O of the linked coordinate system [1] at the center of gravity [2]

In this case, we will assume that the absolute angular velocity of rotation of the trihedron xxxyr in space is equal to y and is directed along the axis [3]

To determine the position of the gyrostabilizer elements, we introduce the following coordinate systems:

1. Coordinate system [4] associated with the outer frame of the gimbal, oriented in such a way that the direction of the axis [5] coincides with the direction of the axis of the outer frame of the gimbal, the axis is [6] with the axis of the inner frame, the axis is [7] perpendicular to the first two and forms a right trihedron with them.

2. Coordinate systems [8] associated with the inner frame of the gimbal and the platform, in the initial position coinciding with the axes [9].

The position of the platform relative to the aircraft body is determined by the angles of [10] its rotation relative to the axes and, [11] respectively.

On the platform of the gyrostabilizer (Fig. VIII. 13) there are three gyroscopes with two degrees of freedom with kinetic moments Ni [12] stabilizing the platform relative to the axes [13]

The angles of rotation of gyroscopes with kinetic moments [14] around the precession axes are denoted by [15].

The moments of inertia of the frame of the gimbal of the stabilizer relative to the axes are [16] denoted by the [17] moments of inertia of the inner frame of the gimbal relative to the axes [18] through [19] and the moments of inertia of the platform relative to the axes [20] through, [21] respectively. The moments of inertia of the gyroscopes relative to the precession axes will be denoted by The [22] projections of the absolute angular velocity of the platform rotation on the axis will be [23] denoted by [24]

We believe that the moments of external forces acting around the axes of the gimbal have the following values:

$$M_{x_н} = -D_\alpha\dot{\alpha} + J'_\alpha\ddot{\alpha} + M_{\alpha p} + M_{x_н}^{н.б};$$

$$M_{y_2} = -D_\beta\dot{\beta} + M_{\beta p} + M_{y_2}^{н.б} + J_\beta\omega_{yн} - J'_\beta(\dot{\omega}_{x_3}\sin\varepsilon + \dot{\omega}_{y_3}\cos\varepsilon);$$

$$M_{z_1} = -D_\varepsilon\dot{\varepsilon} + M_{\varepsilon p} + M_{z_3}^{н.б} + J_\varepsilon\dot{\omega}_{z_2} - J'_\varepsilon\dot{\omega}_{z_3};$$

where [25] are the specific damping moments acting around the axes of the gimbal of the gyrostabilizer;

[26] - moments of inertia of the unloading motor rotor, determined relative to the axes of the gimbal of the gyro stabilizer (for absolute rotation of the platform);

[27] - moments of inertia of the unloading motor rotor, determined relative to the axes of the gimbal (for portable rotation of the base);

[28] - inertial moments arising from the imbalance of the platform.

The signals [29] taken from the gyroscopes precession angle sensors [30] after passing the coordinate converter are fed to the unloading motors of the stabilization axes.

The equations of the moments acting with respect to the stabilization axes will be

$$\left.\begin{aligned}
&(A_2+J_\alpha)\left(\frac{\dot{\omega}_{x_3}\cos\varepsilon_0-\dot{\omega}_{y_3}\sin\varepsilon_0}{\cos\beta_0}\right)+B_1(\dot{\omega}_{x_3}\cos\varepsilon_0-\\
&-\omega_{y_3}\sin\varepsilon_0)\cos\beta_0+A\dot{\omega}_{x_3}\cos\beta_0\cos\varepsilon_0-B\dot{\omega}_{y_3}\cos\beta_0\times\\
&\times\sin\varepsilon_0+(C+J_\varepsilon)(\dot{\omega}_{x_3}\cos\varepsilon_0-\dot{\omega}_{y_3}\sin\varepsilon_0)\,\mathrm{tg}\,\beta_0\sin\beta_0+\\
&+D_\alpha\left(\frac{\dot{\omega}_{x_3}\cos\varepsilon_0-\omega_{y_3}\sin\varepsilon_0}{\cos\beta_0}\right)+D_\varepsilon(\omega_{x_3}\cos\varepsilon_0-\omega_{y_3}\sin\varepsilon_0)\times\\
&\times\mathrm{tg}\,\beta_0\sin\beta_0-H_1\dot{\rho}\cos\beta_0\cos\varepsilon_0+H_2\dot{\sigma}\cos\beta_0\sin\varepsilon_0-\\
&-E_\alpha(\rho\cos\varepsilon_0-\sigma\sin\varepsilon_0)=-(A_2+C_1)\ddot{\gamma}\cos\alpha_0\,\mathrm{tg}\,\beta_0-\\
&-(J'_\alpha+J_\varepsilon)\ddot{\gamma}\cos\alpha_0\,\mathrm{tg}\,\beta_0-(D_\alpha+D_\varepsilon)\dot{\gamma}\cos\alpha_0\,\mathrm{tg}\,\beta_0-\\
&-E_\varepsilon\tau\sin\beta_0+M_{x_н}^{н.б}-M_{z_3}^{н.б}\sin\beta_0;\\
&(A_1+J_\beta)(\dot{\omega}_{x_3}\sin\varepsilon_0+\dot{\omega}_{y_3}\cos\varepsilon_0)+A\dot{\omega}_{x_3}\sin\varepsilon_0+\\
&+B\dot{\omega}_{y_3}\cos\varepsilon_0+D_\beta(\omega_{x_3}\sin\varepsilon_0+\omega_{y_3}\cos\varepsilon_0)-\\
&-H_1\dot{\rho}\sin\varepsilon_0-H_2\dot{\sigma}\cos\varepsilon_0-E_\beta(\rho\sin\varepsilon_0+\sigma\cos\varepsilon_0)=\\
&=J_\beta\ddot{\gamma}\sin\alpha_0+D_\beta\dot{\gamma}\sin\alpha_0+M_{y_2}^{н.б};\\
&(C+J_\varepsilon)\dot{\omega}_{z_3}+D_\varepsilon\omega_{z_3}-H_3\dot{\tau}-E_\varepsilon\tau=J_\varepsilon\frac{\cos\alpha_0}{\cos\beta_0}\ddot{\gamma}+\\
&+D_\varepsilon\frac{\cos\alpha_0}{\cos\beta_0}\dot{\gamma}+M_z^{н.б}.
\end{aligned}\right\}$$

The equations of the moments acting with respect to the precession axes will have the form:

$$\left.\begin{aligned}
&A_3\ddot{\rho}+H_1\omega_{x_3}\cos\rho+H_1\omega_{y_3}\sin\rho=M_\rho^{упр};\\
&A_4\ddot{\sigma}+H_2\omega_{y_3}\cos\sigma-H_2\omega_{x_3}\sin\sigma=M_\sigma^{упр};\\
&A_5\ddot{\tau}+H_3\omega_{z_3}\cos\tau+H_3\omega_{x_3}\sin\tau=M_\tau^{упр},
\end{aligned}\right\}$$

where [31] are the control moments.

Differential equations (VIII.52) and (VIII.53) are a closed system describing, in the first approximation, the motion of a gyrostabilizer installed on an aircraft.

Free movement of the gyro stabilizer without unloading device, provided that [32] is determined by the differential equations

$$\left.\begin{aligned}&[A_2+J_\alpha+B_1\cos^2\beta_0+A\cos^2\beta_0+\\&+(C_1+J_\varepsilon)\sin^2\beta_0]\dddot{\alpha}_{a\delta c}+\\&+(D_\alpha+D_\varepsilon\sin^2\beta_0]\ddot{\alpha}_{a\delta c}+\frac{H^2}{A_0}\cos^2\beta_0\dot{\alpha}_{a\delta c}=0;\\&(A_1+J_\beta+A)\dddot{\beta}_{a\delta c}+D_\beta\ddot{\beta}_{a\delta c}+\frac{H^2}{A_0}\dot{\beta}_{a\delta c}=0;\\&(C+J_\varepsilon)\dddot{\varepsilon}_{a\delta c}+D_\varepsilon\ddot{\varepsilon}_{a\delta c}+\frac{H^2}{A_0}\dot{\varepsilon}_{a\delta c}=0,\end{aligned}\right\}$$

Where [33]

$$\begin{aligned}\dot{\beta}_{a\delta c}&=\omega_{x_3}\sin\varepsilon_0+\omega_{y_3}\cos\varepsilon_0,\\\dot{\varepsilon}_{a\delta c}&=\omega_{z_3},\end{aligned}$$

[34] - components of the absolute angular rate of rotation of the gyrostabilizer platform around the axis of the outer frame of the gimbal, the inner axis and the axis of rotation of the platform.

Frequency of nutation oscillations of the platform relative to the axes of its gimbal

$$\left.\begin{aligned}&n_{н.н}=\frac{H\cos\beta_0}{\sqrt{[A_2+J_\alpha+(B_1+A)\cos^2\beta_0+(C_1+J_\varepsilon)\sin^2\beta_0]\,A_0}};\\&n_{н.в}=\frac{H}{\sqrt{(B_1+J_\beta+A)\,A_0}};\quad n_{н.пл}=\frac{H}{\sqrt{(C+J_\varepsilon)\,A_0}}.\end{aligned}\right\}$$

Due to the fact that individual channels of biaxial and triaxial gyrostabilizers in the first approximation can be represented as isolated from each other uniaxial gyro stabilizers, many reasons for the appearance of disturbing moments that generate errors in a single uniaxial gyro stabilizer remain the same for biaxial and triaxial gyro stabilizers.

In particular, taking into account the angular stiffness of gyroscopes by introducing the reduced moments of inertia , the choice of correcting links to ensure the stability of the system, the determination of the components of the own precession velocity [35]For each separate channel of a triaxial

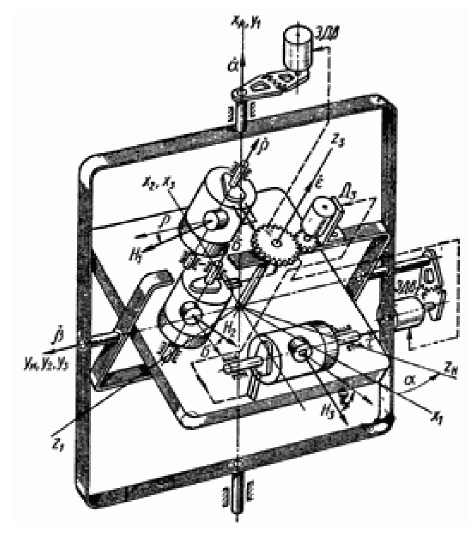


Fig. VIII. 14. Diagram of an indicator power gyro stabilizer

gyro stabilizers are performed in the same way as for a uniaxial stabilizer.

The dynamic components of the intrinsic precession speed of a triaxial gyro is much less than that of a uniaxial or biaxial one, since the portable angular velocity around the rotor of any gyroscope is small due to the platform stabilization in inertial space along all three coordinates. To determine the dynamic error, relations (VIII.45), (VIII.46) can be used.

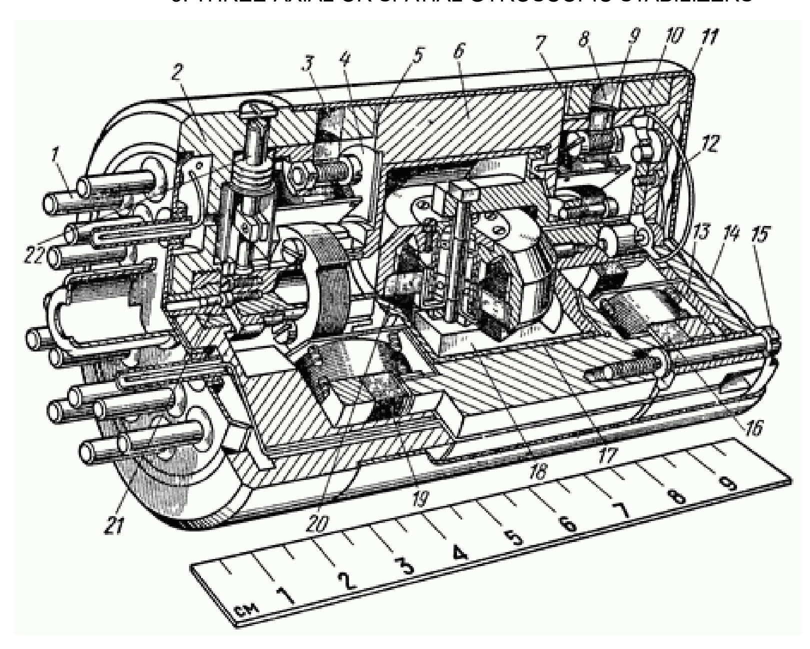


Fig. VIII. 15. Section of the float integrating gyroscope: 1 - plug connector; 2, 6 and 10 - body parts; 3 and 8 - holes for adjusting the position of the stators of the signal and torque sensors; 4 - screen, 5 and 7 - flanges for mounting sensors; 11 - cover; 12 - tape current lead; 13 - washer with current leads; 14 - membrane box; 15 - screws, 16 - torque sensor stator; 17 - float; 18 - gyromotor frame; 19 - signal sensor stator, 20 - gyromotor, 21 - float axis and stone; 22 - device for balancing the float

An important type of perturbations acting on the gyrostabilizer platform and generating its dynamic errors are the moments of external forces arising during angular oscillations of the aircraft [8].

Indicator and power stabilizer. In fig. VIII. 14 shows an indicator gyro stabilizer, sometimes referred to simply as an indicator gyro.

In the indicator-force gyrostabilizer, integrating gyroscopes or

astatic gyroscopes - measuring the angle of rotation of the platform, damping gyroscopes - measuring the angular rate ofrotation of the platform.

Let us consider the features of the formation of a spatial gyroscopic stabilizer circuit with float gyroscopes (Fig. VIII.15). Outwardly, the scheme of such a spatial gyro stabilizer hardly differs from the scheme of the power spatial gyroscopic stabilizer shown in Fig. VII 1.13.

The main difference between the circuits in Fig. VIII. 12 and VIII.13 from the diagram in Fig. VIII. 14 is that the float of the integrating gyroscope is weighed on the platform with the help of a viscous liquid filling the gap between the float and the gyroscope body.

The term "indicator gyrostabilizer" is used here in connection with the fact that float gyroscopic sensors operate in the so-called indicator mode, that is, they only measure the angles of rotation of the gyrostabilizer platform in space, and gyroscopic moments developed by float gyroscopes practically do not participate in the suppression process. moments of external forces acting on the gyrostabilizer platform.

The differential equations of motion of the spatial gyroscopic stabilizer with float gyroscopes have the form

$$\left.\begin{aligned}
&[A_2+J_\alpha+B_1\cos^2\beta_0+(C_1+J_\varepsilon)\sin^2\beta_0+\\
&+A\cos^2\beta_0]\ddot{\alpha}_{\text{абс}}+(D_\alpha+D_\varepsilon\sin^2\beta_0)\dot{\alpha}_{\text{абс}}-\\
&-H\dot{\rho}\cos\varepsilon_0\cos\beta_0+H\dot{\sigma}\sin\varepsilon_0\cos\beta_0=\\
&=-(A_2+C_1)\ddot{\gamma}\cos\alpha_0\,\mathrm{tg}\,\beta_0-(J_\alpha+\\
&+J_\varepsilon)\ddot{\gamma}\cos\alpha_0\,\mathrm{tg}\,\beta_0-(D_\alpha+D_\varepsilon)\dot{\gamma}\cos\alpha_0\,\mathrm{tg}\,\beta_0+\\
&+M_\alpha-M_\varepsilon\sin\beta_0+M_{x_н}^{н.б}-M_{z_3}^{н.б}\sin\beta_0;\\
&(A_1+A+J_\beta)\ddot{\beta}_{\text{абс}}+D_\beta\dot{\beta}_{\text{абс}}-H\dot{\rho}\sin\varepsilon_0-H\dot{\sigma}\cos\varepsilon_0=\\
&=J_\beta\ddot{\gamma}\sin\alpha_0+D_\beta\dot{\gamma}\sin\alpha_0+M_\beta+M_{y_2}^{н.б};\\
&(C+J_\varepsilon)\ddot{\varepsilon}_{\text{абс}}+D_\varepsilon\dot{\varepsilon}_{\text{абс}}-H\dot{\tau}=\\
&=J_\varepsilon\ddot{\gamma}\frac{\cos\alpha_0}{\cos\beta_0}+D_\varepsilon\dot{\gamma}\frac{\cos\alpha_0}{\cos\beta_0}+M_\varepsilon+M_{z_3}^{н.б},
\end{aligned}\right\}$$

Where [36]

[37] - the value of the current in the control windings of the unloading motors;

[38] - the slope of the corresponding characteristics of the electric motors.

The current flowing in the control winding of the electric motor comes from the output stage of the amplifier . Differential Equations ,

determining the change in the current at the amplifier output , we take in the form:

$$\left.\begin{aligned}
T_1\dot{I}_1+I_1&=n_1'u_1;\\
T_2\dot{I}_2+I_2&=n_2'u_2;\\
T_3\dot{I}_3+I_3&=n_3'u_3,
\end{aligned}\right\}$$

where [39] are the time constants of the respective amplifiers. Signal generation [40] corresponds to the expressions:

$$\left.\begin{aligned}
\tilde{U}_1&=W_{\alpha p}^{*}(s)(\rho\cos\varepsilon_0-\sigma\sin\varepsilon_0);\\
\tilde{U}_2&=W_{\beta p}^{*}(s)(\rho\sin\varepsilon_0+\sigma\cos\varepsilon_0);\\
\tilde{U}_3&=W_{\varepsilon p}^{*}(s)\,\tau,
\end{aligned}\right\}$$

where [41] or [42] is the transfer function in the channel unloading circuit [43].

For the simplest proportional characteristic of the unloading device in the absence of correction:

$$W_{\alpha p}^{*}(s)=E_\alpha;\quad W_{\beta p}^{*}(s)=E_\beta;\quad W_{\varepsilon p}^{*}(s)=E_\varepsilon,$$

the motion of the integrating gyroscopes is described by the equations:

$$\left.\begin{aligned}
A_3\ddot{\rho}+D_\rho\dot{\rho}&=-H_1\omega_{x_3}\cos\rho-H_1\omega_{y_3}\sin\rho+M_\rho-A_3\dot{\omega}_{z_3};\\
A_4\ddot{\sigma}+D_\sigma\dot{\sigma}&=-H_2\omega_{y_3}\cos\sigma+H_2\omega_{x_3}\sin\sigma+M_\sigma-A_4\dot{\omega}_{z_3};\\
A_5\ddot{\tau}+D_\tau\dot{\tau}&=-H_3\omega_{z_3}\cos\tau-H_3\omega_{x_3}\sin\tau+M_\tau+A_5\dot{\omega}_{y_3},
\end{aligned}\right\}$$

where [44] are the specific damping moments.

Without correction, the free movement of the gyro, provided that the [45] angle is also [46] relatively small, is determined by three independent differential equations

$$\left.\begin{aligned}
J_0^{\alpha}\ddot{\alpha}_{\text{абс}}+(D_\alpha+iH)\dot{\alpha}_{\text{абс}}+E_\alpha i\alpha_{\text{абс}}&=M_{x_н}^{0};\\
J_0^{\beta}\ddot{\beta}_{\text{абс}}+(D_\beta+iH)\dot{\beta}_{\text{абс}}+E_\beta i\beta_{\text{абс}}&=M_{y_2}^{0};\\
J_0^{\varepsilon}\ddot{\varepsilon}_{\text{абс}}+(D_\varepsilon+iH)\dot{\varepsilon}_{\text{абс}}+E_\varepsilon i\varepsilon_{\text{абс}}&=M_{z_3}^{0},
\end{aligned}\right\}$$

Where

$$J_0^\alpha = A_2 + J_\alpha + (B_1 + A)\cos^2\beta_0 + (C_1 + J_\varepsilon)\sin^2\beta_0;$$
$$J_0^\beta = A_1 + I_\beta + A; \quad J_0^\varepsilon = C + J_\varepsilon;$$

- gear ratio (gear ratio) of the integrating gyroscope.

Static errors of platform stabilization are determined by the ratios:

$$\left.\alpha_{абс}^* = \frac{M_{x_н}^0}{E_\alpha i}; \quad \beta_{абс}^* = \frac{M_{y_2}^0}{E_\beta i}; \quad \varepsilon_{абс}^* = \frac{M_{z_3}^0}{E_\varepsilon i}. \right\}$$

The dynamic errors of the spatial gyroscopic stabilizer with float gyroscopes are determined similarly to the errors of the power gyroscopic stabilizer.

<< Previous paragraph Next paragraph >>